

Synthesis and characterization of porous bentonite adsorbent and its application to remove methylene blue dye from aqueous solutions

Nihed Daas, Hassina Zaghouane-Boudiaf*

Laboratoire de Génie des Procédés Chimiques, Département de Génie des Procédés, Faculté de Technologie, Université Ferhat ABBAS Sétif-1, Sétif 19000, Algeria, Mobile No.: +213661288939; Tel./Fax: +21336 61 11 58; emails: boudiafhassina2000@yahoo.fr/boudiafhassina2000@univ-setif.dz (H. Zaghouane-Boudiaf), daasnihed@yahoo.fr/nihed.daas@univ-setif.dz (N. Daas)

Received 26 September 2021; Accepted 5 January 2022

ABSTRACT

To improve the performance of organophilic clay in water treatment, it was treated with a neutral amine and a source of silica tetraethyl orthosilicate with formula $\text{Si}(\text{OC}_2\text{H}_5)_4$. The obtained materials were called PCHs (porous clay heterostructures). To allow us to better appreciate their properties, PCHs samples were subjected to different characterizations as Fourier-transform infrared spectroscopy, X-ray diffraction and Brunauer–Emmett–Teller analysis, then they were applied in batch reactor adsorption of the model cationic dye methylene blue (MB). The prepared PCHs adsorbents have high affinity towards MB. The most known Langmuir and Freundlich models were applied to analyze experimental isotherm data. The maximum adsorption capacity founded was of 274 and 361 mg/g for the prepared samples. The adsorption mechanism was based on the hydrophobic–hydrophobic interactions. These results are important in selecting the most effective and suitable adsorbent for cationic dyes removal from polluted environments.

Keywords: Porous adsorbent; Dye; Batch adsorption; Porous clay heterostructures; Kinetics; Water treatment

1. Introduction

Porous clay heterostructures (PCHs) are new materials, having favorable features, such as combined micro- and mesopores, large surface area (until 900 m^2/g), high mass transfer rates and high adsorption capacities [1]. The unique structural characteristics give PCHs potential applications as adsorbents [2], catalysts [3,4], carriers [5] and templates [6]. In general, PCHs are synthesized through the organic modification of inorganic clay, the intercalation of tetraethyl orthosilicate (TEOS), and removal of the organic templates by calcination or solvent extraction. To obtain a PCH with desirable surface properties (i.e., particle size and morphology, porous structure, type of active sites) synthesis conditions should be correctly adjusted. Physicochemical properties of these

materials can be regulated through various parameters including nature of the pillaring agent, type of clay, particle size distribution of starting material, pillaring procedure, thermal treatments etc.

Industrial wastewater contains many contaminating organic and inorganic materials, such as metals, aromatic compounds and dyes. They are classified as hazardous pollutants because of their potential toxicity both to human health and environment. The dyes pose significant health threat to humans due to their high carcinogenicity and potential toxicity [7]. Methylene blue is one of such as cited dyes. MB dye is harmful to aquatic organisms. It is therefore necessary to avoid release into the environment. For example for fish, the dose of 40.0 mg/L (96 h) is toxic. For humans MB used at doses below 7 mg/kg is associated with few adverse

* Corresponding author.

effects. However, doses above 7 mg/kg associated with cases of nausea, abdominal pain and confusion [8].

Adsorption has been vastly reported as the most widely used technique for the removal of toxic organic and inorganic pollutants. Several authors have successfully used adsorbents for removal of various environmental pollutants including dyes [9–17], metal ions [18–20] and micropollutants [21,22] from wastewater because of its performance and ease of operations [23,24]. Several clays are used as effective adsorbents. There are many reports about the modified bentonite such as organophilic-bentonite, inorganic-organo-bentonite and acid-activated bentonite. They showed outstanding performance on the separation and removal of pollutants and micropollutants [25–29]. However, until recently, there is some lack of knowledge about the adsorption as an effective method of dyes removal using PCHs as adsorbent. In this study, methylene blue (MB) as a typical dye was used to evaluate the adsorption properties of the prepared PCHs.

2. Materials and methods

2.1. Chemicals

The bentonite (Bent) used in this study was obtained from MAGHNIA (West Algeria). Its chemical composition was found to be: 56.8% SiO₂, 18.5% Al₂O₃, 3.7% MgO, 0.03% MnO, 1.4% K₂O, 0.5% CaO, 2.9% F₂O₃, 1.6% Na₂O, 0.1% TiO₂, 13.6% loss of ignition and its cation exchange capacity (CEC) is of 97 meq/g [30]. Cetyltrimethylammonium bromide (CTAB: C₁₉H₄₂NBr, 99%) and butylamine (BA: C₄H₁₁N, 98%) were purchased from Sigma-Aldrich Chemicals. Tetraethyl orthosilicate (TEOS: Si(OCH₂CH₃)₄, chemically pure), MB, sodium hydroxide (NaOH), hydrochloric acid (HCl) and peroxide (H₂O₂) were purchased from Fluka Chemicals.

2.2. Synthesis of adsorbents “PCHs”

The organo-montmorillonite (OMt) was prepared by the exchange of an amount of CTAB equal to the CEC of montmorillonite (Mt) which is approximately equal to 97 meq/g. The surfactant was dissolved in 1 L of distilled water at 80°C and stirred for 3 h. A total of 10 g of Mt was added to the surfactant solution. The dispersion was stirred for 3 h at 80°C. The separated organo-montmorillonite (OMt) was washed with distilled water. Washing was repeated until the supernatant solution was free of bromide ions, as indicated by the AgNO₃ test. The OMt was oven-dried at 80°C until the water was completely evaporated, grounded and then stored in hermetic bottles until they are used. In the second-step, the PCH precursor was prepared from OMt as follows: the OMt was reacted with butylamine (BA) and a source of silica (TEOS) at OMt/BA/TEOS molar ratio of 1/20/150 and 1/20/10. The mixture was stirred for 4 h at room temperature. The resulting sample was recovered by filtration and air-dried overnight. The amine molecules were removed from the resulting sample by calcination at 550°C for 6 h in air to produce the PCH-cal. Another route used in PCHs for removing the amine molecules is the extraction using solvents. For this process the PCH was washed with an HCl/Ethanol

solution (0.1 M). It was filtered and air-dried overnight to produce PCH-HCl.

2.3. Characterization of adsorbents

The point of zero charge (pH_{pzc}) was determined according to the method described by Nandi et al. [31]. Briefly, 50 mL of distilled water was adjusted to pH_i from 2 to 12 using 0.1 M HCl or NaOH. Then 0.5 g of adsorbent was added to each solution. Mixtures were agitated for 48 h at room temperature (≈24°C) and the final pH of the solutions (pH_f) was measured. The point of zero charge (pH_{pzc}) was determined by plotting pH_f – pH_i vs. pH_i and the intersection of the x-axis with the curve gives the value of the pH_{pzc}.

Fourier-transform infrared spectroscopy (FTIR) study was carried out using FTIR 8400S Shimadzu having a standard mid-IR DTGS detector. FTIR spectra were recorded, in the range of 400–4,000 cm⁻¹ with KBr pellet technique. Nitrogen gas adsorption-desorption isotherms were measured using a Quanta Chrome Autosorb-1 instrument at 77 K. The measurements were made after degassing under vacuum at 180°C for 6 h. The specific surface area (S.B.E.T) was calculated by the B.E.T method using the adsorption and desorption isotherms, respectively. The total pore volume was calculated from the maximum amount of nitrogen gas adsorption at partial pressure (P/P₀) = 0.999 [32].

2.4. Adsorption studies

Adsorption experiments were carried out in a batch equilibrium mode. The MB concentrations were determined using a UV-1700 UV spectrophotometer at 664 nm. The amount of MB adsorbed was derived from initial and final concentrations of MB in the liquid phases. All experiments were run in triplicate to ensure reproducibility. Isotherms were studied from 100 to 1,200 mg/dm³ initial concentrations at room temperature (T = 24°C ± 1°C) and at pH of the dispersion (MB solution + adsorbent: pH = 6.4). The effects of pH (2 to 11), and initial MB concentration C₀ (50, 100 and 150 mg/dm³) vs. time were investigated. The amount of adsorption at equilibrium, q_e (mg/g) and at time t was calculated using the liquid-phase concentrations of dye at initial time C₀ (mg/dm³), the liquid-phase concentrations of dye at equilibrium and at time (t) respectively C_e and C_t (mg/dm³), the volume of the solution (L) and the mass of dry adsorbent used (g).

3. Results and discussion

3.1. Characterization of adsorbents

Adsorbents used for characterization are PCH-HCl and PCH-cal with OMt/BA/TEOS molar ratio of 1/20/10. The plots of pH_f – pH_i vs. pH_i gave the intersections with the x-axis which are the values of points of zero charge (pH_{pzc}) of the adsorbents (Fig. 1). These values are respectively of 4.9 and 5.0 for PCH-HCl and PCH-cal. This result confirms that PCH-HCl and PCH-cal surfaces are acidic. It well known that acidity is a specific property of PCHs [33]. The precursor of PCHs is OMt and when the prepared adsorbent was washed with HCl or was

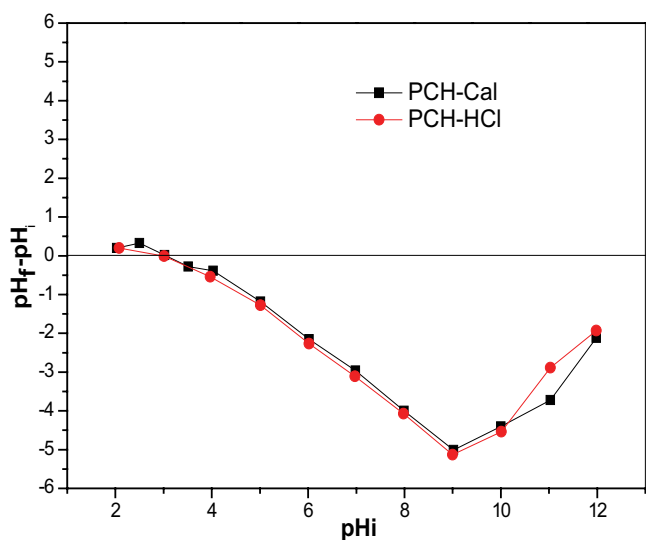


Fig. 1. Isoelectric points of the adsorbents.

calcined the surfactants degrade and thus generate excess protons, which make acidic supports [34].

The FTIR spectra of OMt and PCHs with different treatments were not shown and results are as follow: FTIR spectrum of OMt, PCH-HCl and PCH-cal exhibit band located between 3,200 and 3,800 cm^{-1} (3,630 cm^{-1}) with an intense peak and shoulders around 3,630 and 3,430 cm^{-1} characterizing bentonite. This band corresponds to the elongation vibrations of OH groups of the octahedral layer coordinated at an aluminum or magnesium atom, or else two aluminum atoms. The band located at 2,924 cm^{-1} and at 2,869 cm^{-1} corresponds to the antisymmetric (ν_{as} (CH_2)) and symmetric (ν_{s} (CH_2)) vibration mode of CH_2 respectively. The appearance of two bands between 2,800 and 3,000 cm^{-1} correspond to the CH_3 and CH_2 groups showing the insertion of the surfactant CTAB in the montmorillonite. Intensity of these two bands decreases from spectrum of OMt to PCH-HCl and PCH-cal. This is because in the case of washing sample with HCl, part of the surfactant was dissolved by HCl and the surfactant was degraded when the sample was calcined. The band centered at 1,639 cm^{-1} is attributed to the deformation vibrations of the water molecules adsorbed between the sheets. The intense band located between 900–1,200 cm^{-1} and centered at 1,060 cm^{-1} corresponds to the valence vibrations of the Si–O bond. The two bands in the PCH-HCl spectrum shift from 1,060 to 1,077 and from 1,113 to 1,202 cm^{-1} . The different bands at 915, 844 and 793 cm^{-1} decreased in intensity or disappeared completely on the PCH-HCl spectrum. This is due to the partial dissolution of Fe, Mg and Al caused by the acid wash. During the acid wash, the mechanism proposed by [35] would be as: when the PCH is brought into contact with the acid solution, the interfoliar cations compensating for the negative charges of the layers (in our case it is the alkylammonium ions) are progressively replaced by the abundant H^+ ions in the acid solution to maintain the neutrality clay. The octahedral AlOH groups are simultaneously protonated in AlOH_2^+ , in particular those located at the edge of the layers. These protonated groups are very unstable which causes the dissolution of the octahedral

Al^{3+} . This phenomenon resulted in the decrease of aluminum ions and the disappearance of the frequency bands associated with Si–O–Al and Al–OH–Al on the PCH-HCl spectrum. The vacancy left by the octahedral ions released into the solution leaves access to the acid to attack the deeper ions of the tetrahedral layers of the clay particles, depending on whether the acid is strong or weak. The band at 3,449 cm^{-1} and the intense band centered at 1,621 cm^{-1} corresponds to the elongation vibrations of the NH groups and to deformation vibrations of the butylamine compound respectively. The intense band centered at 1,041 cm^{-1} corresponds to the C–N elongation vibrations. The intense band centered at 806 cm^{-1} corresponds to the N–H deformation vibrations.

The N_2 adsorption/desorption isotherms of the heterostructured samples (Figure not showed) gave results as follow: the isotherm of PCH-HCl and PCH-cal are type IV according to the IUPAC classification [32] suggesting higher porosity. An increase in the quantity of the adsorbed volume at relative pressures ($P/P_0 < 0.02$) indicates micropores. The upward deflection of the pressure of 0.02 to 0.3 and the quasi-linear portion in approximate relative pressures of 0.05 to 0.25 are an indication of mesopores having sizes in the small area of mesopores or in the super-micropore region (between 15 and 25 Å). Based on these characteristics, PCHs are the only materials that combine micro and mesoporosity. This is confirmed by the values of the porous volumes found [34]. In addition, the layered textural character of the base clay was preserved, which was manifested by the unchanged H_3 hysteresis loop of the curves for PCHs. Results of texture parameters of the samples are given in Table 1 where a_{BET} is the surface BET, a_{ext} is the external surface, a_{int} is the internal surface, V_{T} is the total volume of porous, V_{micro} is the volume of the microporous; V_{meso} is the volume of mesoporous and Av diameter is the average diameter of the pores.

From this table, we see that the specific surface area of Mt increases from 80 to 297 and 448 m^2/g respectively for PCH-cal and PCH-HCl. The same results are found by Aguiar et al. [2]. We can also see that the porous volumes increase considerably for heterostructured materials, from 0.048 (Mt) to 0.418 and 0.463 respectively for PCH-HCL and PCH-cal.

3.2. Adsorption isotherm studies

Adsorption isotherm is very important in describing the relationship between the adsorbate and adsorbent. Moreover, by isotherm analysis, the adsorption capacity of the adsorbent, which is an important parameter in the industrial design for adsorption process, is predicted. The Langmuir and Freundlich isotherm models were used to determine the MB adsorption isotherm parameters on the PCHs templates. The Langmuir model [36] explains the monolayer adsorption process that occurs on the homogeneous adsorbent surface, whereas the Freundlich isotherm [37] presumes that the multilayer of the adsorption process occurs on a heterogeneous surface. The nonlinear form of Freundlich [Eq. (2)] and Langmuir [Eq. (3)] isotherm models can be described by the following equations, respectively:

$$q_e = K_f C_e^{1/n} \quad (1)$$

Table 1
Experimental data from textural studies of PCHs with molar ratio OMt/BA/TEOS of 1/20/10

Sample	Mnt-Na	PCH-HCl	PCH-cal
a_{BET} (m ² /g)	10.00	448	297
a_{ext} (m ² /g)	9.00	110	213
a_{int} (m ² /g)	1.00	338	84
V_{pT} (cm ³ /g)	0.048	0.418	0.463
V_{micro} (cm ³ /g)	0	0.198	0.370
V_{meso} (cm ³ /g)	0.049	0.230	0.093
Av. diameter (Å)	19	37	62

$$q_e = \frac{q_m K_L C_e}{1 + K_L C_e} \quad (2)$$

where K_f is the Freundlich adsorption coefficient and n is the exponential coefficient that is related to the adsorption intensity, q_m (mg/g) is the Langmuir maximum adsorption capacity of the adsorbent and K_L is the Langmuir's constant related to the adsorption energy.

The applicability of these two models was evaluated by the R^2 values. The highest R^2 values determine the best isotherm model followed by this study.

To know the effect of the ratio OMt/BA/TEOS and treatment on adsorption capacities of prepared samples, isotherm study was investigated and results are shown in Fig. 2. For the same initial MB concentrations of 100–1,200 mg/dm³, the experimental maximum adsorption capacities are of 361 and 274 mg/g respectively for the PCH-HCl (washed with HCl/ethanol) and PCH-cal with molar ratio of 1/20/10. It was of 175 and 146 mg/g respectively for the PCH-HCl and PCH-cal with molar ratio of 1/20/150. From these results, the high adsorption capacity is attributed to the PCH-HCl adsorbent prepared with OMt/BA/TEOS molar ratio of 1/20/10 (361 mg/g) and to the PCH-cal adsorbent prepared with OMt/BA/TEOS molar ratio of 1/20/10 (274 mg/g). From the obtained results, we can conclude that the molar ratio influenced more on the adsorption capacity. Fig. 2B and C show that the PCH prepared with the molar ratio OMt/BA/TEOS 1/20/10 had adsorption capacity higher (two times) than the adsorption capacity of the PCH prepared with molar ratio OMt/BA/TEOS of 1/20/150. This tendency can be explained by sample which was treated with more silica TEOS became more organophobic and adsorbs less organic dye MB. Fig. 4A shows the effect of treatment used to remove surfactants. The surfactants were removed using calcination at 600°C (PCH-cal) and washing with solvent HCl/ethanol (PCH-HCl). From this figure we can see that adsorption capacity of PCH-HCl is greater than PCH-cal. This is due to the fact that when PCHs were calcined the surfactants were completely removed at 600°C, but extraction with solvent generates a remaining amount of surfactant present in the pores. In this case PCH-HCl is more organophilic than PCH-cal, so adsorbs more organic dye MB.

Adsorption isotherms are of type L according to the classification of Gilles characterized by the electrostatic

interaction between adsorbate and adsorbent surfaces. High affinity is observed from the low concentrations. Sample's adsorption capacity increases with increasing initial concentration until attains equilibrium to form plateau.

To calculate maximum adsorption capacities of samples, Langmuir and Freundlich models were applied using non linear form of Eqs. (1) and (2). Parameters of the two models are given in Table 2. The maximum adsorption capacities of samples founded by Langmuir model are reasonably similar to $q_{e,\text{exp}}$ and the values of R^2 ($0.977 \leq R^2 \leq 0.993$) are higher than that of Freundlich model ($0.882 \leq R^2 \leq 0.956$). These results showed that isotherms were well described by Langmuir model with the monolayer and the homogeneous distribution of the adsorbates on the surfaces of the adsorbents.

Based on the preliminary assessment of the different adsorbents in terms of the experimental and calculated maximum adsorption capacity, PCH-HCl and PCH-cal with molar ratio 1/20/10 were the best adsorbents among the samples tested. Therefore, all further experiments were performed using PCH-HCl and PCH-cal with molar ratio 1/20/10.

3.3. Effect of initial pH on the adsorption of MB onto PCH-cal and PCH-HCl

The initial pH is a very important parameter in adsorption because it can change: (1) the surface charge of the adsorbent, (2) the degree of ionization of the adsorbate and (3) the degree of dissociation of the functional groups of the active sites of the adsorbent [31]. The pKa of MB is of 3.8, so at pH > 3.8, MB is ionized (99% at pH = 6.5). In the same time our samples have two behaviors according the pH value. In acidic medium, pH less than pH_{pzc} , our samples are positively charged, in medium where pH higher than pH_{pzc} (pH_{pzc} of 4.9 and 5), they are negatively charged. In this case there are strong attraction between positive MB ions and negative surfaces of adsorbents. From Fig. 3, it can be seen that there is no variation in the adsorbed amount of MB on the two samples. It can be said that there are no pH effect in the studied pH variation.

3.4. Effect of the adsorbent mass

The effect of adsorbent mass on the adsorption was studied by varying the mass from 10 to 100 mg with 20 mL volume of MB solution, which gives adsorbent concentrations ranging from 0.5 to 5 g/dm³. Fig. 4 shows that the removal of MB by the two adsorbents increases with increasing the adsorbent mass until reaching total elimination of the dye with only 40 mg of PCH-HCl (2.5 g/dm³) with an initial MB concentration of 300 mg/dm³, then the removal of MB remained constant. For PCH-cal, the total elimination of MB dye was observed for PCH-cal mass of 100 mg. This phenomenon can be explained by the specific surface area of adsorbents which are very different. Specific surface area of PCH-HCl (448 m²/g) is greater (1.5 times) than the PCH-cal specific surface area which is 297 m²/g. It well known that the adsorbent surface increases with increasing the adsorbent mass. In this case for having total removal of MB by PCH-cal with the same concentration (300 mg/dm³), it is

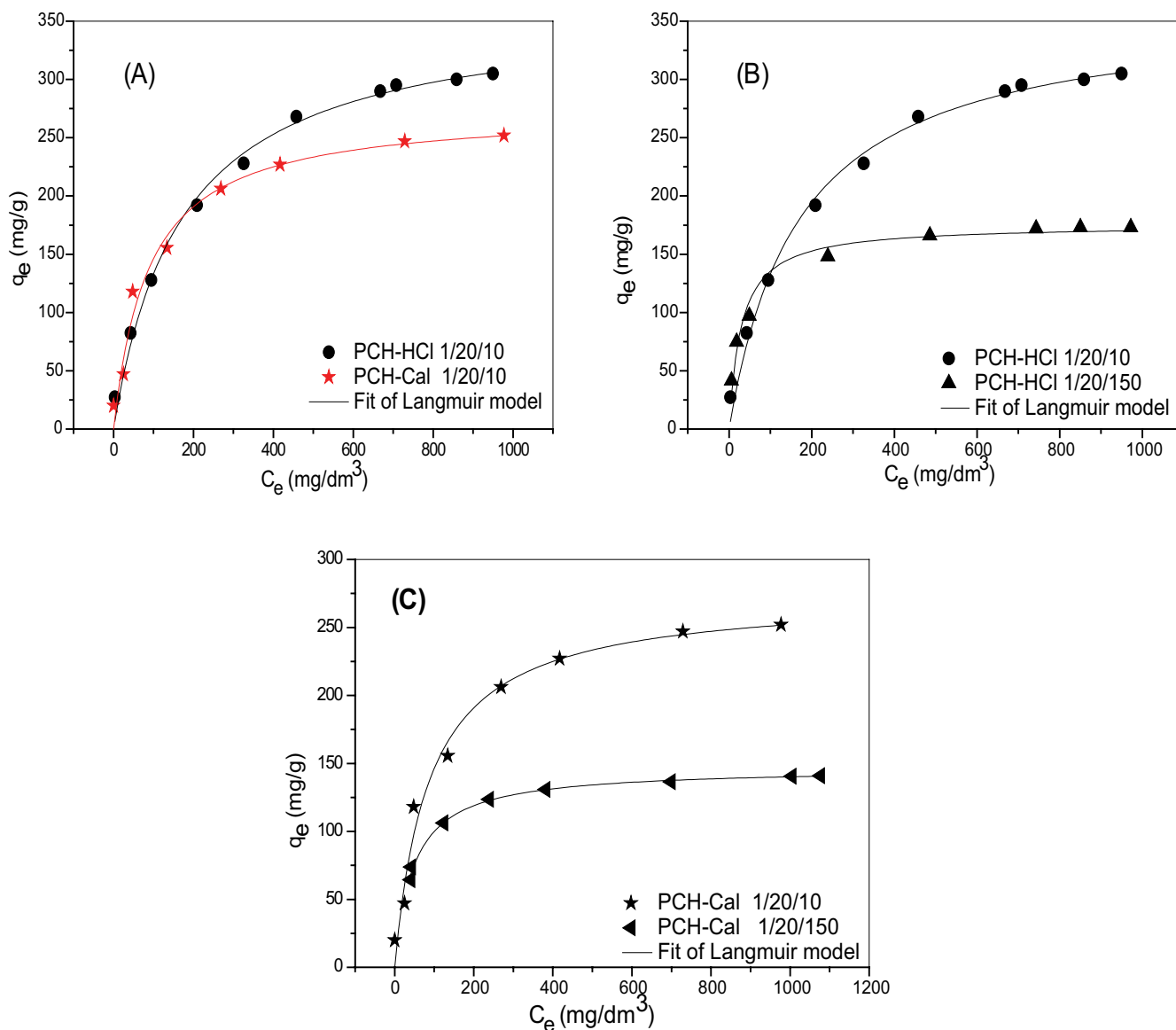


Fig. 2. Isotherms of adsorption of MB onto samples: (A) effect of treatment to remove organic compounds and (B) and (C) effect of molar ratio OMT/BA/TEOS.

Table 2
Langmuir and Freundlich isotherm parameters for adsorption of MB onto samples with two molar ratio and two treatments

OMt/BA/TEOS molar ratio	1/20/10			1/20/150		
Langmuir parameters	Q_{max}	K_L	R^2	Q_{max}	K_L	R^2
PCH-HCl	361.21	0.006	0.991	175.28	0.034	0.972
PCH-cal	274.12	0.011	0.993	146.72	0.002	0.977
Freundlich parameters	K_f	n	R^2	K_f	n	R^2
PCH-HCl	36.21	0.34	0.918	38.28	0.22	0.956
PCH-cal	75.34	0.15	0.882	38.46	0.19	0.917

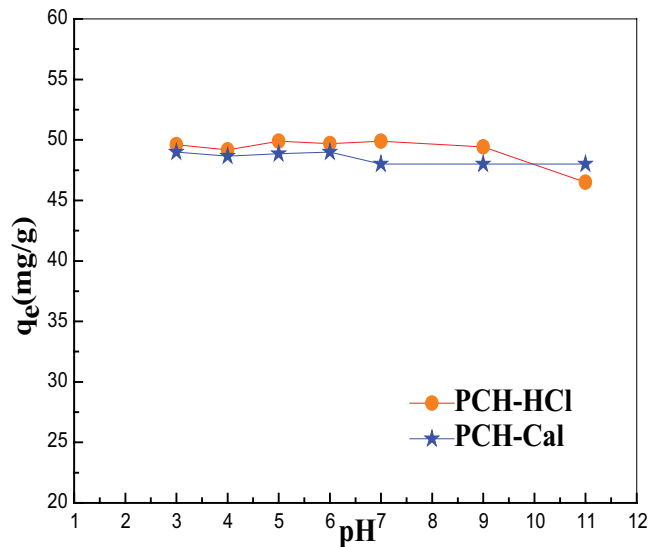


Fig. 3. Effect of the initial pH solution on the adsorption of MB onto PCH-HCl and PCH-cal ($C_0 = 50 \text{ mg/dm}^3$; $V = 20 \text{ mL}$; $m = 20 \text{ mg}$; $T = 23^\circ\text{C} \pm 1^\circ\text{C}$; contact time = 2 h).

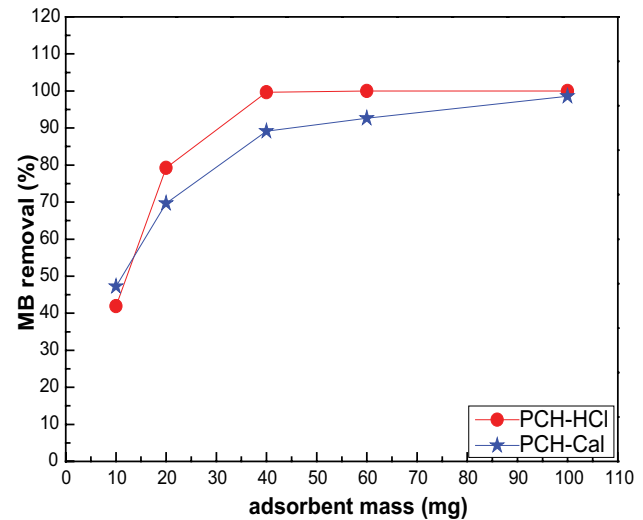


Fig. 4. Effect of adsorbent dosage on removal of MB by PCH-HCl and PCH-cal ($C_0 = 300 \text{ mg/dm}^3$; $V = 20 \text{ mL}$; $T = 23^\circ\text{C} \pm 1^\circ\text{C}$; contact time = 2 h).

Table 3
Kinetic parameters of adsorption of MB onto samples

	C_0	$q_{e,exp}$	Pseudo-first-order				Pseudo-second-order			
			$q_{e,cal}$	k_1	R^2	RMSE	$q_{e,cal}$	k_2	R^2	RMSE
PCH-HCl	50	47	47.41	0.667	0.746	0.711	47.81	0.1050	0.993	1.047
	100	99	96.50	0.178	0.834	1.125	102.78	0.0030	0.982	2.918
	150	140	135.54	0.078	0.917	2.441	152.60	0.0006	0.979	2.476
PCH-cal	50	32.01	30.36	0.223	0.678	5.594	32.32	0.0128	0.997	3.152
	100	62.84	59.96	0.224	0.844	1.199	63.70	0.0058	0.991	0.214
	150	96.17	91.85	0.204	0.923	1.947	97.76	0.0042	0.954	31.319

k_1 (1/min), k_2 (g/mg min), $q_{e(exp,cal)}$ (mg/g), C_0 (mg/dm³)

necessary to increase the adsorption surface, so it is necessary to increase PCH-cal mass.

3.5. Adsorption kinetic and modeling

A kinetic study has a great significant consideration in the adsorption process as it offers information about adsorption and mass transfer mechanism. It helps to determine the time necessary to obtain equilibrium of adsorption. For this, the adsorption kinetics was investigated using initial concentrations of 50, 100 and 150 mg/dm³ and results are given in Fig. 5. The obtained curves showed, as the initial concentration of the solution increases, the adsorbed amounts also increase. From the appearance of the curves, it can be said that there is a great affinity between the MB and the samples studied. The amount of MB adsorbed increased gradually when initial concentration of MB increases from 50 to 150 mg/dm³ until equilibrium. The equilibrium time was reached quickly for low concentrations (40–60 min) contrary to

the high concentrations, the equilibrium contact times were 120 to 160 min. For the first few minutes, the existence of free sites on the surface of the adsorbent allows a rapid fixation of the adsorbate molecules. This step is followed by diffusion to less accessible sites before reaching an adsorption balance where all sites will be occupied. Having low contact equilibrium time is very important in adsorption processes. It reduces the cost and energy of the process and makes it very interesting.

The pseudo-first and pseudo-second-order models were employed to correlate the kinetics data. The pseudo-first-order kinetics model was suggested by Lagergren [38] for adsorption of solid/liquid systems and can be expressed by non-linear form as:

$$q_t = q_e \left(1 - \exp^{-k_1 t}\right) \quad (3)$$

where q_e and q_t are the adsorption amounts at equilibrium and at time t (min) respectively, and k_1 (1/min) is the rate constant of pseudo-first-order adsorption.

The nonlinear form of pseudo-second-order kinetic model can be expressed as [39]:

$$q_t = \frac{q_e^2 k_2 t}{1 + q_e k_2 t} \tag{4}$$

where k_2 (g/mg min) is the rate constant for the second-order kinetic model.

Nonlinear regression has been shown to be better than linear regression such that more realistic values of q_e and k values, and often a higher correlation coefficient (R^2) value are obtained. During nonlinear regression, model parameters are first estimated and then continuously evolve toward the values that minimize a predefined error function [40].

The pseudo-first and pseudo-second-order kinetic parameters determined at $24^\circ\text{C} \pm 1^\circ\text{C}$ are presented in Table 3. The coefficient correlation R^2 and the root-mean squared error (RMSE) were used to ascertain the applicability of the models. The RMSE and R^2 can be determined by the following equations:

$$R^2 = 1 - \frac{\sum_{n=1}^n (q_{t,\text{exp},n} - q_{t,\text{cal},n})^2}{\sum_{n=1}^n (q_{t,\text{exp},n} - \overline{q_{t,\text{exp},n}})^2} \tag{5}$$

$$\text{RMSE} = \sqrt{\frac{1}{n-1} \sum_{n=1}^n (q_{t,\text{exp},n} - q_{t,\text{cal},n})^2} \tag{6}$$

From Table 3 we can see that the high correlation coefficient (R^2) values showed that adsorptions of MB onto PCHs are well described by the pseudo-second-order model. Moreover the values of $q_{e,\text{exp}}$ are reasonably similar to $q_{e,\text{cal}}$ and RMSE values are very low. The value of k_2 decreases from $1,051 \times 10^{-4}$ to 6.88×10^{-4} g/mg min with increasing initial concentration from 50 to 150 mg/dm³.

3.6. Adsorption mechanism

The intraparticle diffusion is another model of kinetics to determine the reaction rate of MB adsorption on adsorbents. The kinetic data of MB sorption onto PCHs were fitted into Morris–Weber intraparticle diffusion. Its equation can be written as follows [41]:

$$q_t = K_{\text{id}} \times t^{0.5} + C \tag{7}$$

Eq. (7) is an empirical equation where adsorbed quantity q_t varies proportionally with $t^{0.5}$ rather than with t , K_{id} is the rate constant of intraparticle diffusion expressed

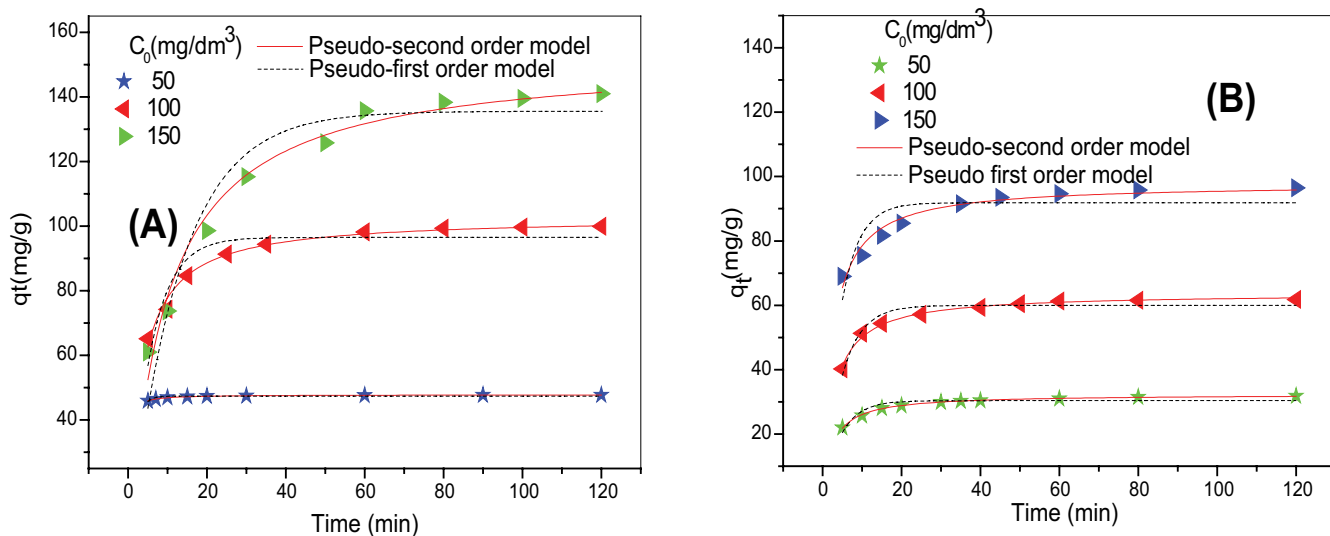


Fig. 5. Effect of contact time and initial concentration in the adsorption of MB: (A) on the sample PCH-HCl and (B) on the sample PCH-cal ($V_{\text{sol}} = 50$ mL; adsorbent mass = 50 mg; agitation speed = 100 rpm; $T = 24^\circ\text{C} \pm 1^\circ\text{C}$, $\text{pH}_{\text{sol}} = 6.4$ (not adjusted)).

Table 4
Intraparticle diffusion parameters for adsorption of MB onto PCH-HCl and PCH-cal

C_0	PCH-HCl				PCH-cal			
	Step1		Step2		Step1		Step2	
	K_{id}	R^2	K_{id}	R^2	K_{id}	R^2	K_{id}	R^2
50	0.155	0.592	0.155	0.591	2.428	0.886	0.351	0.941
100	9.736	0.958	1.424	0.856	8.759	0.887	0.039	0.777
150	13.500	0.968	1.589	0.966	6.216	0.966	1.303	0.932

C (mg/dm³), K_{id} (mg g⁻¹ min^{-0.5})

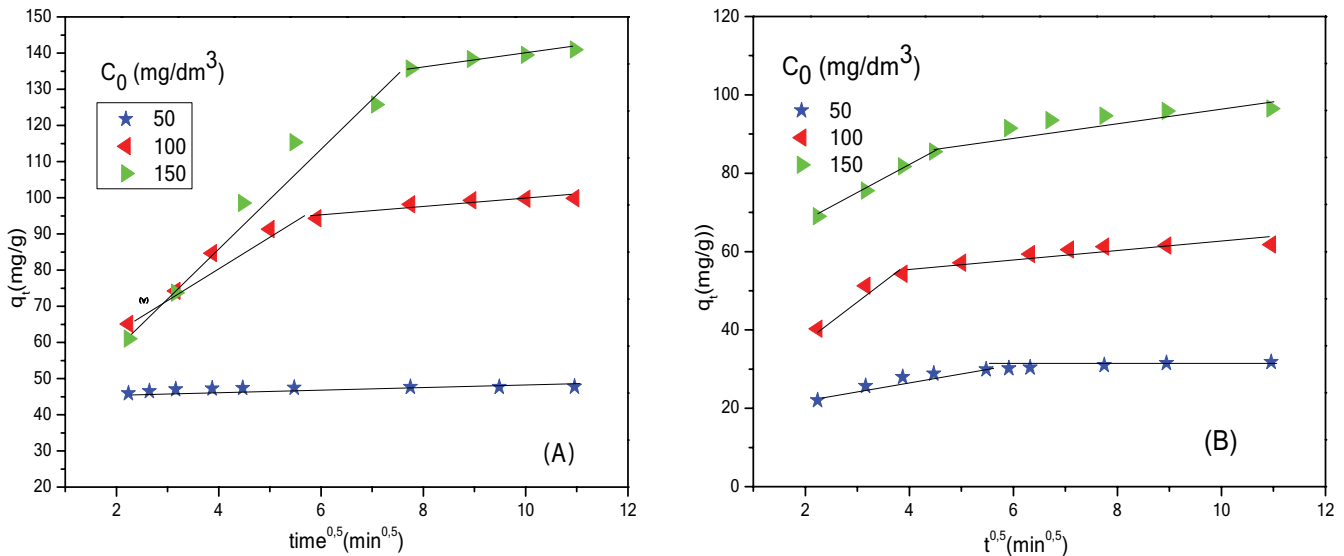


Fig. 6. Weber and Morris intraparticle diffusion plot for the removal of MB by: (A) PCH-HCl and (B) PCH-cal at $24^{\circ}\text{C} \pm 1^{\circ}\text{C}$.

Table 5
Comparison of monolayer MB adsorption onto various adsorbents

Adsorbents	Maximum monolayer adsorption capacities (mg/g)	References
Porous clay heterostructures PCH-HCl	361	This study
Porous clay heterostructures PCH-cal	274	This study
Jackfruit peel	286	[43]
Charred citrus fruit peel	26	[44]
Activated banana peel	20	[45]
Activated carbon produced from buriti shells	274	[46]
Activated lemon peels	208	[47]
Glutamic acid modified chitosan magnetic	180	[48]

in $\text{mg/g min}^{0.5}$ obtained by tracing q_i according to $t^{0.5}$. Fig. 6A and B show the results. The linearity of the data in q_i vs. $t^{0.5}$ plot ensured the intraparticle diffusion process mechanism. Based on Fig. 6 and the low R^2 values for the intraparticle diffusion model presented in Table 4, the plots are non-linear for the whole range of concentrations studied, indicating that intraparticle diffusion is not the only rate-limiting step, but other process may also be involved in the adsorption process. Two different stages are clearly observed in Fig. 6. The first stage describes the instant adsorption which can be attributed to external surface adsorption. In this stage the MB molecules are transported to the external surface through film diffusion and rate of adsorption is very fast. This rapid and instantaneous adsorption is due to the large surface area and the low competition between the dye molecules. The second-part describes the slow adsorption stage caused by the low concentration gradients and the final stage to the adsorption reaction for attained the equilibrium conditions [42].

4. Conclusion

This study showed that the synthesized PCHs had important adsorption capacity for the adsorption of MB dye. The results showed that the MB adsorption was dependent on initial concentration, contact time, and not on initial pH solution. The MB adsorption kinetic and equilibrium data at various process parameters were analyzed using the non-linear equations. The obtained results indicated the good applicability of pseudo-second-order kinetic model according to the high R^2 values and low values of RMSE. Weber's intraparticle diffusion model indicated that two steps have taken place during the adsorption process. The intraparticle diffusion was not the rate-limiting step. The experimental equilibrium data were fitted well to Langmuir model with $0.977 \leq R^2 \leq 0.993$ and monolayer adsorption capacity of 361.21 and 274.12 mg/g.

We have also studied adsorption of MB onto commercial activated carbon (AC) (DARCO) and we found that adsorption capacity of AC is of 111.68 mg/g. Compared to

the adsorption capacity of the prepared PCHs, we have concluded that PCHs are more efficient and they are potential adsorbents for the removal of MB and other cationic dyes.

References

- [1] Y. Wang, P. Zhang, K. Wen, X. Su, J. Zhu, H. He, A new insight into the compositional and structural control of porous clay heterostructures from the perspective of NMR and TEM, *Microporous Mesoporous Mater.*, 224 (2016) 285–293.
- [2] J.E. Aguiar, J.A. Cecilia, P.A.S. Tavares, D.C.S. Azevedo, E. Rodríguez-Castellón, S.M.P. Lucena, I.J. Silva Jr., Adsorption study of reactive dyes onto porous clay heterostructures, *Appl. Clay Sci.*, 135 (2017) 35–44.
- [3] R. Sanchis, J.A. Cecilia, M.D. Soriano, M.I. Vázquez, A. Dejoj, J.M. López Nieto, E. Rodríguez Castellón, B. Solsona, Porous clays heterostructures as supports of iron oxide for environmental catalysis, *Chem. Eng. J.*, 334 (2018) 1159–1168.
- [4] L. Chmielarz, A. Kowalczyk, M. Skoczek, M. Rutkowska, B. Gil, P. Natkański, M. Radko, M. Motak, R. Dębek, J. Ryczkowski, Porous clay heterostructures intercalated with multicomponent pillars as catalysts for dehydration of alcohols, *Appl. Clay Sci.*, 160 (2018) 116–125.
- [5] N. Bunnak, S. Ummartyotin, P. Laoratanakul, A.S. Bhalla, H. Manuspiya, Synthesis and characterization of magnetic porous clay heterostructure, *J. Porous Mater.*, 21 (2014) 1–8.
- [6] C. Santos, M. Andrade, A.L. Vieira, A. Martins, J. Pires, C. Freire, A.P. Carvalho, Templated synthesis of carbon materials mediated by porous clay heterostructures, *Carbon*, 48 (2010) 4049–4056.
- [7] J. Mittal, Recent progress in the synthesis of layered double hydroxides and their application for the adsorptive removal of dyes: a review, *J. Environ. Manage.*, 295 (2021) 113017.
- [8] A. Charbonneau, Toxicité sérotoninergique résultant d'une interaction médicamenteuse entre le bleu de méthylène et les inhibiteurs de la recapture de la sérotonine, *Can. J. Hosp. Pharm.*, 66 (2013) 241–252.
- [9] V.K. Gupta, S. Agarwal, R. Ahmad, A. Mirza, J. Mittal, Sequestration of toxic Congo red dye from aqueous solution using ecofriendly guar gum/activated carbon nanocomposite, *Int. J. Biol. Macromol.*, 158 (2020) 1310–1318.
- [10] S. Soni, P.K. Bajpai, D. Bharti, J. Mittal, C. Arora, Removal of crystal violet from aqueous solution using iron based metal organic framework, *Desal. Water Treat.*, 205 (2020) 386–399.
- [11] J. Mittal, A. Mariyam, F. Sakina, R.T. Baker, A.K. Sharma, A. Mittal, Batch and bulk adsorptive removal of anionic dye using metal/halide-free ordered mesoporous carbon as adsorbent, *J. Cleaner Prod.*, 321 (2021) 129060, doi: 10.1016/j.jclepro.2021.129060.
- [12] A. Mariyam, J. Mittal, F. Sakina, R.T. Baker, A.K. Sharma, A. Mittal, Efficient batch and fixed-bed sequestration of a basic dye using a novel variant of ordered mesoporous carbon as adsorbent, *Arabian J. Chem.*, 14 (2021) 103186, doi: 10.1016/j.arabjc.2021.103186.
- [13] S. Soni, P.K. Bajpai, J. Mittal, C. Arora, Utilisation of cobalt doped Iron based MOF for enhanced removal and recovery of methylene blue dye from waste water, *J. Mol. Liq.*, 314 (2020) 113642, doi: 10.1016/j.molliq.2020.113642.
- [14] A. Mariyam, J. Mittal, F. Sakina, R.T. Baker, A.K. Sharma, Adsorption behaviour of Chrysoidine R dye on a metal/halide-free variant of ordered mesoporous carbon, *Desal. Water Treat.*, 223 (2021) 425–433.
- [15] A. Patel, S. Soni, J. Mittal, A. Mittal, C. Arora, Sequestration of crystal violet from aqueous solution using ash of black turmeric rhizome, *Desal. Water Treat.*, 220 (2021) 342–352.
- [16] A. Umar, M.S. Khan, S. Alam, I. Zekker, J. Burlakovs, S.S. dC Rubin, G.D. Bhowmick, A. Kallistova, N. Pimenov, M. Zahoor, Synthesis and characterization of Pd-Ni bimetallic nanoparticles as efficient adsorbent for the removal of Acid Orange 8 present in wastewater, *Water*, 13 (2021) 1095, doi: 10.3390/w13081095.
- [17] D. Humelnicu, E.S. Dragan, M. Ignat, M.V. Dinu, A comparative study on Cu²⁺, Zn²⁺, Ni²⁺, Fe³⁺, and Cr³⁺ metal ions removal from industrial wastewaters by chitosan-based composite cryogels, *Molecules*, 25 (2020) 2664, doi: 10.3390/molecules25112664.
- [18] A. Zh. Baimenov, D.A. Berillo, K. Moustakas, V.J. Inglezakis, Efficient removal of mercury(II) from water by use of cryogels and comparison to commercial adsorbents under environmentally relevant conditions, *J. Hazard. Mater.*, 399 (2020) 123056, doi: 10.1016/j.jhazmat.2020.123056.
- [19] D. Zhang, K. Zhang, X. Hu, Q. He, J. Yan, Y. Xue, Cadmium removal by MgCl₂ modified biochar derived from crayfish shell waste: batch adsorption, response surface analysis and fixed bed filtration, *J. Hazard. Mater.*, 408 (2021) 124860, doi: 10.1016/j.jhazmat.2020.124860.
- [20] G.K. Gupta, M.K. Mondal, Mechanism of Cr(VI) uptake onto sagwan sawdust derived biochar and statistical optimization via response surface methodology, *Biomass Convers. Bioref.*, (2020), doi: 10.1007/s13399-020-01082-5.
- [21] A.S. Khan, T.H. Ibrahim, M.I. Khamis, P. Nancarrow, J. Iqbal, I. AlNashef, N. Abdel Jabbar, M.F. Hassan, F.S. Mjalli, Preparation of sustainable activated carbon-alginate beads impregnated with ionic liquid for phenol decontamination, *J. Cleaner Prod.*, 321 (2021) 128899, doi: 10.1016/j.jclepro.2021.128899.
- [22] G. Derafa, H. Zaghoulane-Boudiaf, New eco-friendly composite beads from biomass activated carbon for removal of highly toxic 2,4-dichlorophenol from aqueous medium: equilibrium, modeling and thermodynamic studies, *Desal. Water Treat.*, 209 (2021) 324–333.
- [23] C. Zhou, Q. Wu, T. Lei, I.I. Negulescu, Adsorption kinetic and equilibrium studies for methylene blue dye by partially hydrolyzed polyacrylamide/cellulose nanocrystal nanocomposite hydrogels, *Chem. Eng. J.*, 251 (2014) 17–24.
- [24] L. Obeid, N. El Kollli, N. Dali, D. Talbot, S. Abramson, M. Welschbillig, V. Cabuil, A. Bée, Adsorption of a cationic surfactant by a magisorbent based on magnetic alginate beads, *J. Colloid Interface Sci.*, 432 (2014) 182–189.
- [25] S. Ismadi, D.S. Tong, F.E. Soetaredjo, A. Ayucitra, W.H. Yu, C.H. Zhou, Bentonite hydrochar composite for removal of ammonium from Koi fish tank, *Appl. Clay Sci.*, 114 (2015) 467–473.
- [26] A. Aichour, H. Zaghoulane-Boudiaf, Highly brilliant green removal from wastewater by mesoporous adsorbents: kinetics, thermodynamics and equilibrium isotherm studies, *Microchem. J.*, 146 (2019) 1255–1262.
- [27] D. Garmia, H. Zaghoulane-Boudiaf, C. Viseras Ibhora, Preparation and characterization of new low cost adsorbent beads based on activated bentonite encapsulated with calcium alginate for removal of 2,4-dichlorophenol from aqueous medium, *Int. J. Biol. Macromol.*, 115 (2018) 257–265.
- [28] N. Belhouchat, H. Zaghoulane-Boudiaf, C. Viseras, Removal of anionic and cationic dyes from aqueous solution with activated organo-bentonite/sodium alginate encapsulated beads, *Appl. Clay Sci.*, 135 (2017) 9–15.
- [29] E. Baigorria, L.A. Cano, L.M. Sanchez, V.A. Alvarez, R.P. Ollier, Bentonite-composite polyvinyl alcohol/alginate hydrogel beads: preparation, characterization and their use as arsenic removal devices, *Environ. Nanotechnol. Monit. Manage.*, 14 (2020) 100364, doi: 10.1016/j.enmm.2020.100364.
- [30] H. Khalaf, O. Bouras, V. Perrichon, Synthesis and characterization of Al-pillared and cationic surfactant modified Al-pillared Algerian bentonite, *Microporous Mesoporous Mater.*, 8 (1997) 141–150.
- [31] B.K. Nandi, A. Goswami, M.K. Purkait, Adsorption characteristics of brilliant green dye on kaolin, *J. Hazard. Mater.*, 161 (2009) 387–395.
- [32] E.P. Barrett, L.G. Joyner, P.P. Halenda, The determination of pore volume and area distributions in porous substances. I. Computations from nitrogen isotherms, *J. Am. Chem. Soc.*, 73 (1951) 373–380.
- [33] A.J. Schwanke, S.B.C. Pergher, Porous heterostructured clays – recent advances and challenges – revisão, *Cerâmica*, 59 (2013) 576–587.

- [34] F. Kooli, Porous clay heterostructures (PCHs) from Al13-intercalated and Al13-pillared montmorillonites: properties and heptane hydro-isomerization catalytic activity, *Microporous Mesoporous Mater.*, 184 (2014) 184–192.
- [35] T.-H. Wang, T.-Y. Liu, D.-C. Wu, M.-H. Li, J.-R. Chen, S.-P. Teng, Performance of phosphoric acid activated montmorillonite as buffer materials for radioactive waste repository, *J. Hazard. Mater.*, 173 (2010) 335–342.
- [36] I. Langmuir, The constitution and fundamental properties of solids and liquids. Part I. Solids, *J. Am. Chem. Soc.*, 40 (1918) 1361–1403.
- [37] H. Freundlich, Über die adsorption in lösungen, *Z. Phys. Chem.*, 57 (1906) 385–470.
- [38] S. Lagergren, Zur theorie der sogenannten adsorption gelöster stoffe, *Kungliga Svenska Vetenskapsakademiens. Handlingar*, 24 (1898) 1–39.
- [39] Y.S. Ho, G. McKay, Pseudo-second-order model for sorption processes, *Process Biochem.*, 34 (1999) 451–465.
- [40] K.L. Tan, B.H. Hameed, Insight into the adsorption kinetics models for the removal of contaminants from aqueous solutions, *J. Taiwan Inst. Chem. Eng.*, 74 (2017) 25–48.
- [41] W.J. Weber, J.C. Morris, *Water Pollution Symposium*, Proc. Int. Conf. Pergamon, Oxford, 1962, pp. 231–266.
- [42] B. Assia, Md. A. Islam, H. Zaghouane-Boudiaf, M. Boutahala, B.H. Hameed, Calcium alginate–bentonite–activated carbon composite beads as highly effective adsorbent for methylene blue, *Chem. Eng. J.*, 270 (2015) 621–630.
- [43] B.H. Hameed, Evaluation of papaya seeds as a novel non-conventional low-cost adsorbent for removal of methylene blue, *J. Hazard. Mater.*, 162 (2009) 344–350.
- [44] S. Dutta, A. Bhattacharyya, A. Ganguly, S. Gupta, S. Basu, Application of Response Surface Methodology for preparation of low-cost adsorbent from citrus fruit peel and for removal of methylene blue, *Desalination*, 275 (2011) 26–36.
- [45] K. Amela, M.A. Hassen, D. Kerroum, Isotherm and kinetics study of biosorption of cationic dye onto banana peel, *Energy Procedia*, 19 (2012) 286–295.
- [46] O. Pezoti Jr., A.L. Cazetta, I.P.A.F. Souza, K.C. Bedin, A.C. Martins, T.L. Silva, V.C. Almeida, Adsorption studies of methylene blue onto ZnCl₂-activated carbon produced from buriti shells (*Mauritia flexuosa* L.), *J. Ind. Eng. Chem.*, 20 (2014) 4401–4407.
- [47] A. Amina, H. Zaghouane-Boudiaf, C. Viseras Iborra, M. Sanchez Polo, Bioadsorbent beads prepared from activated biomass/alginate for enhanced removal of cationic dye from water medium: kinetics, equilibrium and thermodynamic studies, *J. Mol. Liq.*, 256 (2018) 533–540.
- [48] H. Yan, H. Li, H. Yang, A. Li, R. Cheng, Removal of various cationic dyes from aqueous solutions using a kind of fully biodegradable magnetic composite microsphere, *Chem. Eng. J.*, 223 (2013) 402–411.